

A Printed Vivaldi Antenna with Improved Radiation Patterns by Using Two Pairs of Eye-Shaped Slots for UWB Applications

Kun Ma, Zhi Qin Zhao*, Jiang Niu Wu, Mubarak S. Ellis, and Zai Ping Nie

Abstract—In this paper, a printed Vivaldi antenna with two pairs of eye-shaped slots is proposed for UWB applications. By using two pairs of eye-shaped slots, the side lobe levels of the radiation pattern are reduced, and the antenna gain is improved at low frequencies. To illustrate the effectiveness of the proposed design, a prototype of the proposed antenna is fabricated and measured. Experimental results show that the proposed antenna presents a measured impedance bandwidth, defined by $|S_{11}| < -10$ dB, from 3 to 12.8 GHz with a compact size (36 mm × 36 mm). Good unidirectional radiation characteristics with a front-to-back ratio better than 10 dB are also achieved. The measured gain is better than 3.7 dBi in the operating frequency band. In addition, the measured group delay of the proposed antenna is around 1.2 ns with a variation less than ± 0.5 ns.

1. INTRODUCTION

In recent years, ultra-wideband (UWB) technologies have received extensive attention for high-speed wireless communication, biological microwave imaging, and ground penetrating radar (GPR) due to their merits of high-speed data rate, low power dissipation, high precision ranging, and low cost. This results in a need of printed broadband antennas used for ultra wideband (UWB) applications. A variety of UWB antennas have been proposed and investigated. Some printed UWB antennas have gained a lot of recognition due to their advantages of compact structure, small size and ease of integration with other RF circuits. Vivaldi antenna [1–6] has been widely studied in UWB antenna research owing to the merits of low profile, wide impedance bandwidth, moderately high gain, good directivity, benign time-domain characteristics, and symmetric beam both in E -plane and H -plane. However, Vivaldi antenna always needs a large size to achieve good performance.

With the aim to reduce the size of Vivaldi antenna and maintain its good performance, a variety of modified Vivaldi antennas have been studied. A modified Vivaldi antenna based on regular slot edge (RSE), loaded lens and choke slot structures is presented in [7]. The low-end operating frequency is extended to lower frequency band, and the radiation patterns at the high frequencies are improved. However, this antenna cannot operate over the entire UWB frequency band. A novel tapered slot edge (TSE) structure is proposed in [8]. This antenna presents wide impedance bandwidth and excellent directive radiation patterns by using the TSE structure. However, this antenna also needs a relatively large size to realize good performance. In [9], an antipodal Vivaldi antenna with good time-domain characteristics is described. This antenna has a very small size, and the impedance bandwidth can cover the entire UWB frequency band. However, the directivity of the antenna is not good, and the gain is low at the low frequencies. Inhomogeneous and anisotropic (IA) zero-index meta-materials (ZIM) are introduced to improve the gain and directivity in [10]. As a result, the antenna has good performance of high gain, good directivity, and wide bandwidth. However, it is difficult to fabricate by etching dielectric materials in the aperture. Corrugations are applied to improve the radiation characteristics of Vivaldi

Received 30 April 2014, Accepted 10 June 2014, Scheduled 14 July 2014

* Corresponding author: Zhi Qin Zhao (zqzhao@uestc.edu.cn).

The authors are with the School of Electronic Engineering, University of Electronic Science and Technology of China, Chengdu, Sichuan 611731, China.

antennas [11–13]. A coplanar waveguide to coplanar stripline transition structure and corrugations are used in [11, 12]. Ultra wideband impedance bandwidth and good directivity are achieved in these antennas. However, these antennas also have large sizes. In [13], a small Vivaldi antenna with variable-length corrugations is presented. The directive radiation characteristics of this antenna are improved by using variable-length corrugations. However, a substrate with high dielectric constant is used to achieve the similar size to my design using a low dielectric substrate.

In this paper, a compact printed Vivaldi antenna with two pairs of eye-shaped slots is proposed for UWB applications. By using the eye-shaped slots, the surface currents on the outer edges of the antenna can be decreased. The side lobe levels of the radiation pattern can be reduced. This implies that good unidirectional radiation patterns with a high gain are obtained by using a compact size ($36 \text{ mm} \times 36 \text{ mm}$). Measured results of a fabricated prototype verify the effectiveness of the proposed antenna. The measured impedance bandwidth of the proposed antenna, defined by $|S_{11}| < -10 \text{ dB}$, ranges from 3 to 12.8 GHz, which covers the entire UWB frequency band. The size of the proposed antenna is smaller than the antennas in [7, 8, 14].

2. ANTENNA DESIGN AND ANALYSIS

A design procedure to improve the radiation patterns of the Vivaldi antenna using two pairs of eye-shaped slots is illustrated in Figure 1. Firstly, an original Vivaldi antenna, which is used as a reference antenna as shown in Figure 1(a), is designed. This antenna is printed on an FR4 substrate (dielectric constant = 4.4, loss tangent = 0.02) with a thickness of 0.8 mm. This antenna consists of a microstrip-to-slotline transition structure, a radiating slot, and a microstrip feeding line. The size of the substrate is $36 \text{ mm} \times 36 \text{ mm}$. The exponential curves used in the Vivaldi antenna are described as

$$x = \pm c_1 \cdot \exp(r_1(y - 6)) \mp (c_1 - c_2), \quad (6 \text{ mm} \leq y \leq 36 \text{ mm}), \quad (1)$$

where x is the distance from the central axis to the exponential edge, varying from 0.16 to 10 corresponding to y varying from 6 to 36. c_1 , c_2 , and r_1 are equal to 0.31, 0.16, and 0.118, respectively.

Radiation patterns of the original antenna in E -plane and H -plane at 4 GHz are shown in Figure 2. It is observed from Figure 2(a) that the original antenna has high side lobe levels in 0° and 180° directions. The level of the back radiations is also very high. This is caused by the surface currents on the outer edges as shown in Figure 3(a), which are the main contributors to the side lobes [15]. The performance of the antenna can be improved by decreasing the currents on the outer edges. Aiming to decrease the currents on the outer edges, a pair of symmetrical eye-shaped slots are introduced and etched in the top fins. Figure 1(b) shows the structure of the modified Vivaldi antenna. The modified antenna is named as Type-A in this paper. The E-shaped slot consists of two exponential curves: E_1 and E_2 . The exponential curves can be described as

$$E_1: x = 1.4 \cdot \exp(0.16(y - L_1)) + W/2 - W_{s1} - 1.4, \quad (L_1 \leq y \leq L_1 + L_3) \quad (2)$$

$$E_2: y = 1.8 \cdot \exp(0.11(x - W/2 + W_{s1})) + L_1 - 1.8, \quad (W/2 - W_{s1} \leq x \leq W/2). \quad (3)$$

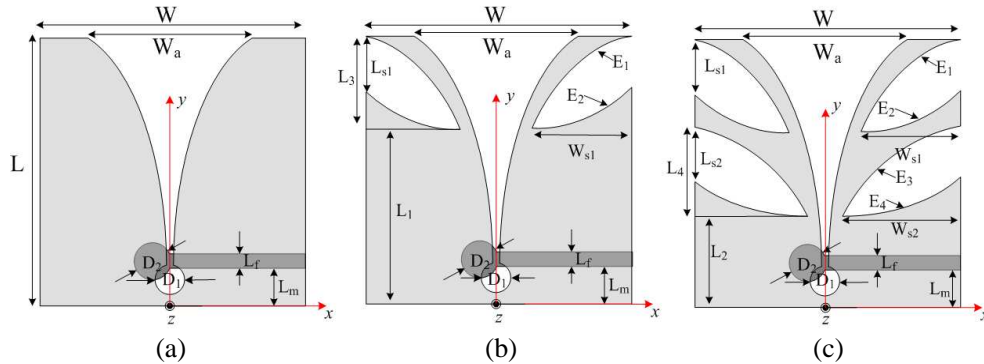


Figure 1. Evolution of the proposed antenna configuration: (a) original design, (b) Type-A, and (c) Type-B.

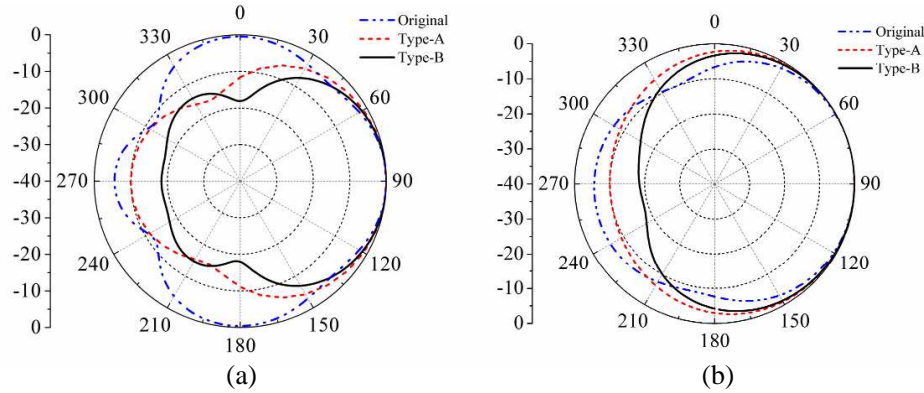


Figure 2. Simulated radiation patterns of original antenna, Type-A, and Type-B at 4 GHz in (a) E -plane and (b) H -plane.

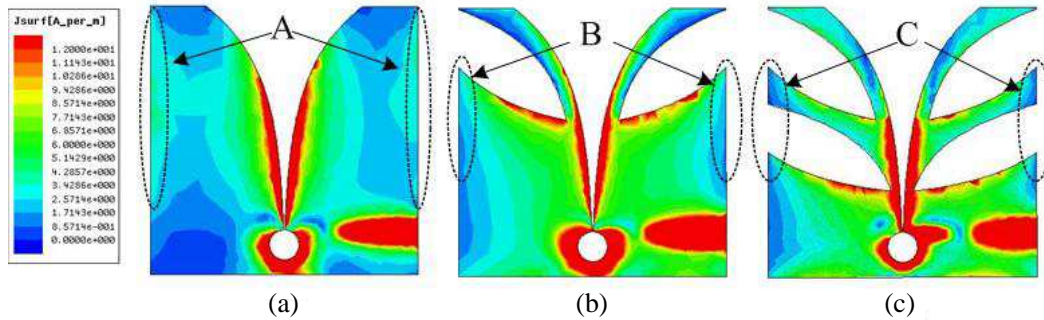


Figure 3. Simulated surface current distribution at 4 GHz of (a) original antenna, (b) Type-A, and (c) Type-B.

As shown in Figure 3(b), and compared with Figure 3(a), the currents on the outer edges are decreased by using the eye-shaped slots, then the side lobe levels of the radiation pattern are reduced as shown in Figure 2. The effects of the eye-shaped slots on reflection coefficient and antenna gains are shown in Figure 5. It is observed that the impedance matching at the low frequencies is improved and a wide bandwidth can be obtained. Also, by using one pair of eye-shaped slots, the gain of Type-A is improved within most of the operating frequency band except the frequency band from 4 to 5 GHz. The gain from 3 to 4 GHz is improved by a value of over 3 dBi. If we continue to increase the size of the eye-shaped slots, the impedance matching will be getting worse.

As shown in Figure 2, the level of the back radiations of the Type-A antenna is still high. This is because the currents in the area of B of the outer edges are still strong as shown in Figure 3(b). Therefore, we adopt another pair of symmetrical eye-shaped slots further to decrease the currents in the area of B to further reduce the side lobe levels without deteriorating the performance of the antenna. Figure 1(c) shows the structure of the modified Vivaldi antenna with two pairs of symmetrical eye-shaped slots. It is named as Type-B in this paper. The additional E-shaped slot consists of two exponential curves: E_3 and E_4 . The exponential curves can be described as

$$E_3: x = 1.8 \cdot \exp(0.2(y - L_3)) + W/2 - W_{s2} - 1.8, \quad (L_2 \leq y \leq L_2 + L_4) \quad (4)$$

$$E_4: y = 1.1 \cdot \exp(0.12(x - W/2 + W_{s2})) + L_2 - 1.1, \quad (W/2 - W_{s2} \leq x \leq W/2). \quad (5)$$

Compared with Figure 3(b), it can be noticed from Figure 3(c) that the currents in the area of C are further decreased. Therefore, the level of the back radiations is significantly reduced due to the additional eye-shaped slots. This phenomenon can be found in Figure 2. In order to illustrate the effects of the two pairs of E-shaped slots to the radiation patterns at the high frequencies, the simulated

radiation patterns both in E -plane and H -plane of the original antenna and Type-B at 7.5 GHz are shown in Figure 4. It is observed that the side lobe levels are significantly reduced in E -plane. Significant improvement in directivity is achieved compared with the original antenna. However, the radiation pattern in H -plane is slightly changed. The radiation pattern of the Type-B is even worse in 195° and 345° direction compared with the original antenna. These phenomena indicate that the proposed antenna is more effective at the low frequencies than at the high frequencies.

The effects of the additional eye-shaped slots on reflection coefficient and antenna gains are investigated and shown in Figure 5. It can be seen from Figure 5(a) that the impedance matching of the Type-B antenna is however better than that on Type-A, especially at the high frequencies. Hence, by using two pairs of eye-shaped slots, ultra wideband performance is achieved. The gain is noticed to be significantly improved when the two pairs of eye-shaped slots are introduced, especially at the low frequencies. Compared with the original antenna and the Type-A antenna, the gain of the Type-B antenna is further improved from 3 to 5 GHz with the value better than 5 dBi. From the above, by using the two pairs of eye-shaped slots, the side lobe levels of the radiation pattern are reduced, good directivity, a moderately high gain and ultrawideband performance are achieved.

Since the E-shaped slots are a critical part in the proposed antenna, a geometric study of the E-shaped slots is investigated. The effects of parameters L_2 and W_{s1} on input impedance of the proposed antenna are simulated and shown in Figure 6. Figure 6(a) shows the simulated reflection coefficients of the proposed antenna with different values of L_2 . It is observed that the impedance matching at the high frequencies is sensitive to the changes of L_1 . The impedance matching is getting better as L_1 increases

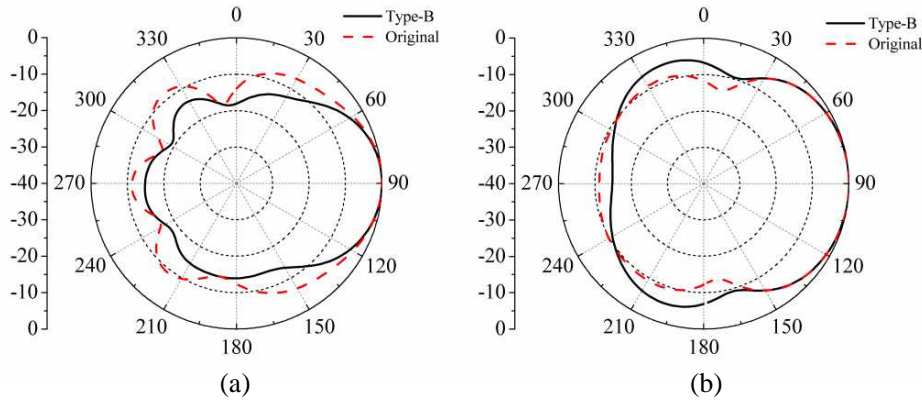


Figure 4. Simulated radiation patterns of original antenna and Type-B at 7.5 GHz in (a) E -plane and (b) H -plane.

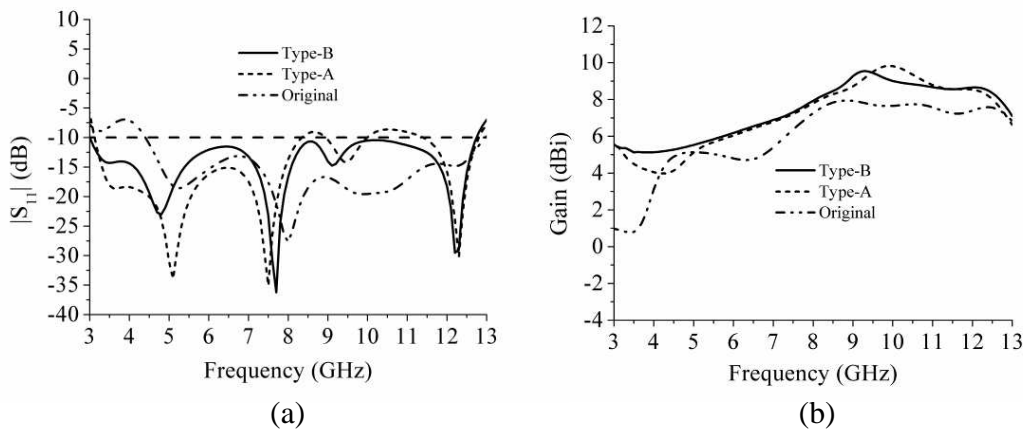


Figure 5. Simulated reflection coefficients and antenna gains of the proposed antennas.

from 10.5 to 11.5 mm. However, as L_1 further increases from 11.5 to 12.5 mm, the impedance matching is getting worse. Figure 6(b) shows the simulated reflection coefficients of the proposed antenna with different values of W_{s1} . As shown in Figure 6(b), it can be seen that the lower-edge frequency is changing from 3.1 to 2.8 GHz corresponding to the variation of W_{s1} from 13.5 to 15.5 mm. The impedance matching at the high frequencies is also changed as W_{s1} changes. When the value of W_{s1} is too big or small, the proposed antenna has poor impedance matching at the high frequencies.

During the optimization phase, the dimensions of the antenna are optimized. The final optimal dimensions of the Type-B antenna are specified as follows: $L = 36$ mm, $L_1 = 21$ mm, $L_2 = 11.5$ mm, $L_3 = 14.8$ mm, $L_4 = 11.6$ mm, $W = 36$ mm, $W_a = 20$ mm, $W_{s1} = 14.5$ mm, $W_{s2} = 16.5$ mm, $D_1 = 4$ mm, $D_2 = 4.8$ mm, $L_f = 1.46$ mm, $L_m = 5.02$ mm, $L_{s1} = 7.7$ mm, $L_{s2} = 6.5$ mm.

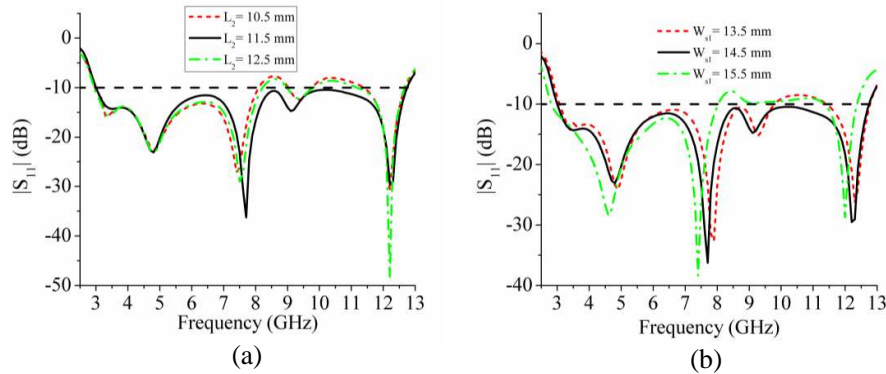


Figure 6. Simulated reflection coefficients of the proposed antenna with different values of (a) L_2 and (b) W_{s1} .

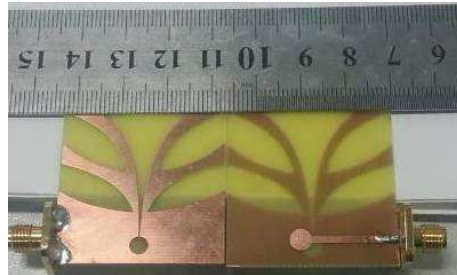


Figure 7. Photographs of the fabricated antenna.

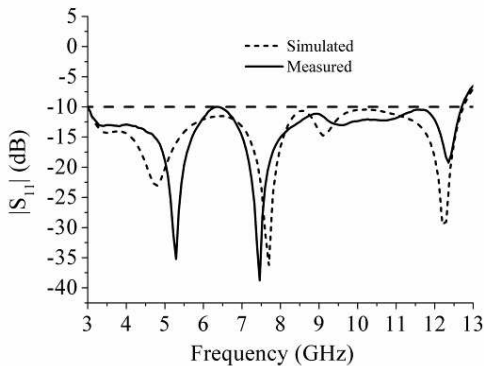


Figure 8. Simulated and measured reflection coefficient of the proposed antenna.

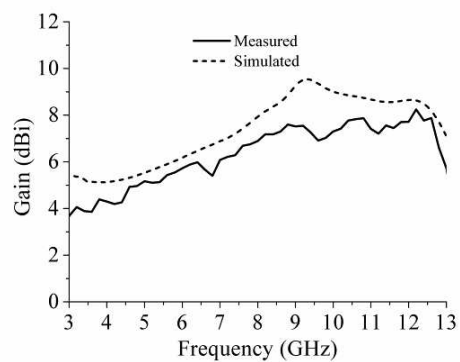


Figure 9. Simulated and measured gain of the proposed antenna.

3. EXPERIMENTAL RESULTS

The proposed antenna was fabricated with the optimized parameters. The photographs of the fabricated antenna are shown in Figure 7. The antenna performance is obtained by using an Agilent E8363B performance network analyzer (PNA) and SATIMO measurement system.

Figure 8 shows the simulated and measured reflection coefficient results of the proposed antenna. It is observed that the measured and simulated results agree well with each other. According to the measured results, the proposed antenna provides a wide impedance bandwidth, defined by $|S_{11}| < -10$ dB, from 3 to 12.8 GHz, which covers the entire UWB frequency band. It indicates that the proposed antenna can realize wideband performance with a compact size ($36 \text{ mm} \times 36 \text{ mm}$). The

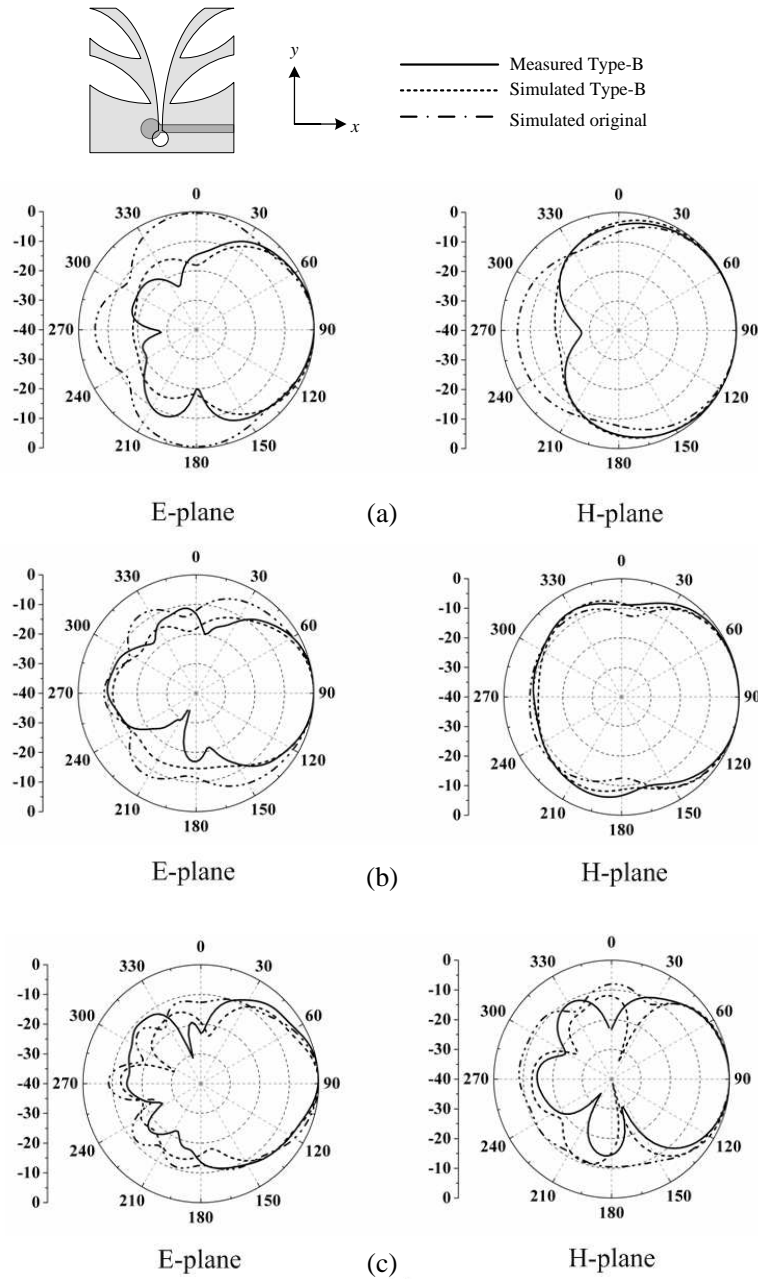


Figure 10. Simulated and measured radiation patterns of the Type-B antenna both in E -plane (xoy -plane) and H -plane (yo z -plane) at: (a) 4 GHz, (b) 7 GHz, and (c) 10 GHz.

differences between the measured and simulated results may be caused by the attached SMA connector and the inaccuracy in fabrication. Figure 9 shows the realized peak gain variation versus frequency of the proposed antenna. The realized peak gain is obtained by using a SATIMO measurement system. The measured results are in good agreement with the simulated results. According to the measured results, the realized gain varies from 3.7 to 8.3dBi within the operating frequency band. The discrepancy between the measured and simulated results may be caused by the substrate loss and measurement error.

The simulated and measured radiation patterns of the Type-B antenna in *E*-plane (*xoy*-plane) and *H*-plane (*yo_z*-plane) at 4, 7 and 10 GHz are shown in Figure 10. In addition, the simulated radiation patterns of the original antenna are also added in Figure 10 for comparison. As shown in the figure, the measured results of the Type-B antenna are in good agreement with the simulated results. The Type-B antenna has good unidirectional radiation patterns and the main lobes are fixed in the endfire direction (*y*-axis direction) within the effective bandwidth. Compared with the original antenna, significant decrease of the side lobe levels is observed at 4 GHz. At 7 GHz, the measured results of the Type-B antenna show that the side lobe levels in *E*-plane are significantly reduced, significant improvement in directivity is achieved compared with the original antenna. However, the radiation pattern of the Type-B in *H*-plane is similar to the original antenna. The radiation pattern of the Type-B is even slightly worse in 0° and 195° direction. At 10 GHz, it is observed from Figure 10(c) that the side lobe levels in *H*-plane are reduced. While the radiation pattern is slightly worse in the 315° direction in *E*-plane compared with the original antenna. These phenomena verify the effectiveness of the Type-B antenna. The Type-B antenna is capable of improving the radiation patterns of the antenna by means of reducing the side lobe levels.

Figure 11 shows the simulated and measured F/B ratios of the proposed antenna. It is observed that the measured F/B ratio is better than 10 dB within the operating frequency band from 3 to 12.6 GHz. This validates that the radiation patterns of the proposed antenna exhibit good unidirectional radiation characteristics. The radiation efficiency of the fabricated antenna is also measured and shown in Figure 11. It can be seen that the measured radiation efficiency of the fabricated antenna is around 80% in the frequency band ranging from 3.6 to 12.5 GHz.

Group delay, which measures the waveform distortion in time domain, is an important parameter for an UWB antenna. Therefore, the group delay of the proposed antenna is also studied. In this paper, two identical antennas are placed face to face in the maximum radiation direction (*y*-axis direction) at a distance of 200 mm, which meets the far-field region condition of $r > D^2/\lambda$, where $D = 51$ mm is the diameter of the sphere which contains the structure of the proposed antenna, $\lambda = 23.4$ mm is the wavelength of the higher-edge frequency. One antenna is used to transmit a signal and the other antenna is used to receive the signal. The measured group delay is obtained by using the Agilent E8363B performance network analyzer (PNA). Figure 12 shows the simulated and measured group delay. From

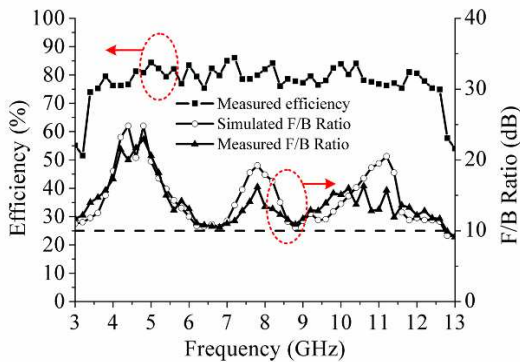


Figure 11. Simulated and measured F/B ratios and measured radiation efficiency of the proposed antenna.

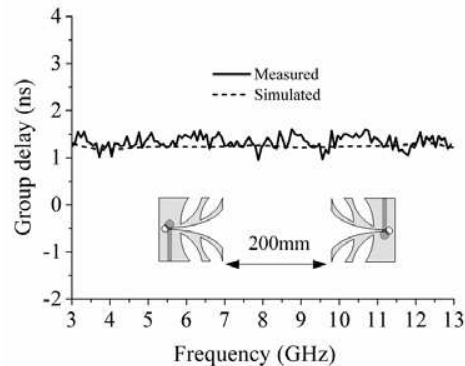


Figure 12. Simulated and measured group delays of the proposed antenna.

this figure, it is observed that the measured results agree well with the simulated results. According to the measured results, the group delay of the proposed antenna is around 1.2 ns in the entire operating frequency band with a variation less than ± 0.5 ns. A relatively flat group delay response is achieved.

4. CONCLUSION

In this paper, a printed Vivaldi antenna with two pairs of eye-shaped slots is designed and experimentally studied for UWB applications. By using two pairs of eye-shaped slots, the side lobe levels of the radiation pattern are reduced, and the gain of the antenna is improved at low frequencies. A wide impedance bandwidth is obtained with a compact size (36 mm \times 36 mm). Experimental results show that the fabricated antenna can operate with a wide impedance bandwidth from 3 to 12.8 GHz and with a moderate gain better than 3.7 dBi. In addition, the radiation patterns of the proposed antenna exhibit good unidirectional radiation characteristics. The measured front-to-back ratio of the fabricated antenna is better than 10 dB in the band 3 to 12.6 GHz. Moreover, the measured group delay of the antenna shows that the proposed antenna has a good time-domain response. Therefore, it is a good candidate for ultrawideband communication systems.

ACKNOWLEDGMENT

This work was supported in part by the National Natural Science Foundation of China by Grants (61171044 and 61231001), the Fundamental Research Funds for the Central Universities of China (ZYGX2012YB010 and ZYGX2012Z005).

REFERENCES

1. Song, Y., Y. C. Jiao, T. L. Zhang, G. Zhao, and F. S. Zhang, "Small tapered slot antenna with a band-notched function for wireless applications," *Progress In Electromagnetics Research*, Vol. 10, 97–105, 2009.
2. Bai, J., S. Y. Shi, and D. W. Prather, "Modified compact antipodal Vivaldi antenna for 4–50 GHz UWB application," *IEEE Trans. Microwave Theory Tech.*, Vol. 59, No. 4, 1051–1057, 2011.
3. Bourqui, J., M. Okoniewski, and E. C. Fear, "Balanced antipodal Vivaldi antenna with dielectric director for near-field microwave imaging," *IEEE Trans. Antennas Propagat.*, Vol. 58, No. 7, 2318–2326, 2010.
4. Yang, Y., Y. Wang, and A. E. Fathy, "Design of compact Vivaldi antenna arrays for UWB see through wall applications," *Progress In Electromagnetics Research*, Vol. 82, 401–418, 2008.
5. Mehdipour, A., K. M. Aghdam, and R. F. Dana, "Completed dispersion analysis of Vivaldi antenna for ultra wideband applications," *Progress In Electromagnetics Research*, Vol. 77, 85–96, 2007.
6. Abbosh, A. M., "Miniaturized microstrip-fed tapered slot antenna with ultra wideband performance," *IEEE Antennas and Wireless Propagat. Lett.*, Vol. 8, 690–692, 2009.
7. Teni, G., N. Zhang, J. H. Qiu, and P. Y. Zhang, "Research on a novel miniaturized antipodal Vivaldi antenna with improved radiation," *IEEE Antennas and Wireless Propagat. Lett.*, Vol. 12, 417–420, 2013.
8. Fei, P., Y. C. Jiao, W. Hu, and F. S. Zhang, "A miniaturized antipodal Vivaldi antenna with improved radiation characteristics," *IEEE Antennas and Wireless Propagat. Lett.*, Vol. 10, 127–130, 2011.
9. Hood, A., Z. T. Karacolak, and E. Topsakal, "A small antipodal Vivaldi antenna for ultra wideband applications," *IEEE Antennas and Wireless Propagat. Lett.*, Vol. 7, 656–660, 2008.
10. Zhou, B., H. Li, X. Y. Zou, and T. J. Cui, "Broadband and high-gain planar Vivaldi antennas based on inhomogeneous anisotropic zero-index metamaterials," *Progress In Electromagnetics Research*, Vol. 120, 235–247, 2011.
11. Xu, H. Y., H. Zhang, J. Wang, and L. X. Ma, "A new tapered slot antenna with symmetrical and stable radiation pattern," *Progress In Electromagnetics Research Letters*, Vol. 5, 35–43, 2008.

12. Wang, N. B., Y. Song, Y. C. Jiao, L. Zhang, and F. S. Zhang, "Extreme wideband tapered slot antenna with impedance bandwidth in excess of 21.6 : 1," *Journal of Electromagnetic Waves and Applications*, Vol. 23, Nos. 2–3, 231–238, 2009.
13. Bialkowski, M. E. and Y. F. Wang, "A size-reduced exponentially tapered slot antenna with corrugations for directivity improvement," *Microwave Conference*, 2482–2485, Singapore, 2009.
14. Lee, D. H., H. Y. Yang, and Y. K. Cho, "Tapered slot antenna with band-notched function for ultra wideband radios," *IEEE Antennas and Wireless Propagat. Lett.*, Vol. 11, 682–685, 2012.
15. Wang, C. J. and T. L. Sun, "Design of a microstrip monopole slot with unidirectional radiation characteristics," *IEEE Trans. Antennas Propagat.*, Vol. 59, No. 4, 1389–1393, 2011.